Theoretical and Applied Fracture Mechanics 17 (1992) 163–175
Elsevier

Inhomogeneous behavior of anti-plane shear crack in softening material with local unloading

T.H. Hao

Department of Basic Science, China Textile University, 1882 West Yan-an Road, Shanghai 200051, People's Republic of China

X.T. Zhang

Institute of Mechanics, Academia Sinica, Beijing 100080, People's Republic of China

K.C. Hwang

Department of Mechanics, Tsinghua University, Beijing 100084, People's Republic of China

Examined in this work is the anti-plane stress and strain near a crack in a material that softens beyond the elastic peak and unloads on a linear path through the initial state. The discontinuity in the constitutive relation is carried into the analysis such that one portion of the local solution is elliptic in character and the other hyperbolic. Material elements in one region may cross over to another as the loading is increased. Local unloading can thus prevail. Presented are the inhomogeneous character of the asymptotic stress and strain in the elliptic and hyperbolic region, in addition to the region in which the material elements had experienced unloading. No one single stress or strain coefficient would be adequate for describing crack instability.

1. Introduction

A material is said to suffer permanent deformation or damage when it surpasses the elastic limit or yield point. Thereafter, the stress and strain response may be nonlinear and unloading would follow a different path. It is customary to pre-assign the same constitutive relation for each element in the system. Inhomogeneity arising from the combined effects of material microstructure, permanent damage and loading is normally neglected. Much of the a priori assumptions may appear to be reasonable for the system behavior at large but they may leave much to be desired in local regions of high stress or energy gradients such as a line of discontinuity or crack.

What can be demonstrated from the classical theory of plasticity is the lack of inhomogeneity of the state of affairs near the crack tip. Such a feature has been shown in past works for in-plane deformation [1–3] and anti-plane shear [4,5]. The character of inhomogeneity depends directly on the assumed form of the constitutive equation. This is reflected in the result of this work in contrast to that in [5] although both dealt with softening materials. Other works related to material damage and softening can be found in [6,7]. One way of not committing to a particular form of the constitutive relation is to provide a scheme where the stress and strain response of each material element is derived [3] rather than preassigned.

2. Basic equations

Under anti-plane shear, all material elements are assumed to deform out of the x_1x_2-plane with u_3 along the x_3-axis being the only non-zero displacement component. Accordingly, only two stress components τ_{13} and τ_{23} prevail with the corresponding strains γ_{13} and γ_{23}. The relations between γ_{i3} and u_3 are:

$$\gamma_{13} = \frac{\partial u_3}{\partial x_1}, \qquad \gamma_{23} = \frac{\partial u_3}{\partial x_2} \tag{1}$$

The resultant shear stress and strain are given by

$$\tau = \sqrt{\tau_{13}^2 + \tau_{23}^2}, \qquad \gamma = \sqrt{\gamma_{13}^2 + \gamma_{23}^2} \tag{2}$$

The assumption of proportional loading then yields

$$\tau_{13} = \frac{\tau}{\gamma}\gamma_{13}, \qquad \tau_{23} = \frac{\tau}{\gamma}\gamma_{23} \tag{3}$$

such that τ_{ij} and γ_{ij} depend only on the space variables x_j ($j = 1, 2$). Equilibrium is enforced by

$$\frac{\partial \tau_{13}}{\partial x_1} + \frac{\partial \tau_{23}}{\partial x_2} = 0 \tag{4}$$

while compatibility is satisfied if

$$\frac{\partial \gamma_{23}}{\partial x_1} - \frac{\partial \gamma_{13}}{\partial x_2} = 0 \tag{5}$$

Solution to a particular problem requires the a priori assumption of the constitutive relation and boundary conditions for a specific geometry and loading.

2.1. Transformation to strain plane

Introduce the function ψ in the complex plane $\gamma_{13} + i\gamma_{23}$ such that eq. (5) is automatically satisfied:

$$x_1 = \frac{\partial \psi}{\partial \gamma_{13}}, \qquad x_2 = \frac{\partial \psi}{\partial \gamma_{23}} \tag{6}$$

Here, x_j are regarded as the dependent variables while γ_{ij} are independent:

$$\gamma_{13} + i\gamma_{23} = \gamma\, e^{i\phi} \tag{7}$$

with ϕ being the argument of γ. Alternatively, x_j can be expressed in terms of γ and ϕ as

$$x_1 = \cos\phi \frac{\partial \psi}{\partial \gamma} - \frac{\sin\phi}{\gamma}\frac{\partial \psi}{\partial \phi}, \qquad x_2 = \sin\phi \frac{\partial \psi}{\partial \gamma} + \frac{\cos\phi}{\gamma}\frac{\partial \psi}{\partial \phi} \tag{8}$$

Because of proportional loading, the stress components can also be written as

$$\tau_{13} + i\tau_{23} = \tau\, e^{i\phi} \tag{9}$$

Application of eq. (4) therefore yields

$$\frac{\tau(\gamma)}{\gamma\tau'(\gamma)}\frac{\partial^2 \psi}{\partial \gamma^2} + \frac{1}{\gamma}\frac{\partial \psi}{\partial \gamma} + \frac{1}{\gamma^2}\frac{\partial^2 \psi}{\partial \phi^2} = 0 \tag{10}$$

in which $\tau'(\gamma) = d\tau/d\gamma$. The anti-plane displacement u_3 is related to ψ as

$$u_3 = \gamma\frac{\partial \psi}{\partial \gamma} - \psi \quad \text{or} \quad \psi = r\frac{\partial u_3}{\partial r} - u_3 \tag{11}$$

with r being the radial distance in a polar coordinate system of the physical plane x_1x_2.

2.2. Constitutive relation

The constitutive relation of the material is displayed graphically in Fig. 1. It has a discontinuity at γ_0 where the shear τ attains its maximum:

$$\tau = G\begin{cases} \gamma, & \text{for } \gamma \leqslant \gamma_0 \\ \gamma_0\sqrt{\dfrac{\gamma_0}{\gamma}}, & \text{for } \gamma \geqslant \gamma_0 \end{cases} \tag{12}$$

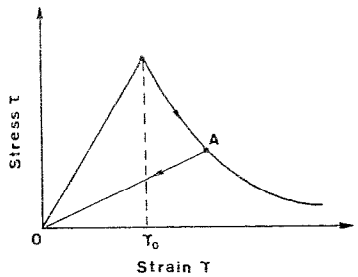

Fig. 1. Stress and strain diagram for material with softening.

Should unloading occur at certain point (r_a, θ_a) in the x_1x_2-plane that corresponds to A in Fig. 1, the stress/strain would follow the straight line A $\rightarrow$ 0 with the modulus $G_t = \tau_t/\gamma_t$. Equation (12) would thus give

$$\frac{G_t}{G} = \left(\frac{\gamma_0}{\gamma_t}\right)^{3/2} \tag{13}$$

3. Semi-infinite crack: solution form

Let a semi-infinite crack occupy the negative portion of the x_1-axis as indicated in Fig. 2. Equations (8) transform the crack in $x_1 + ix_2$ onto the semi-infinite portion of the plane $\gamma_{13} + i\gamma_{23}$ defined by $0 \leqslant \phi \leqslant \pi$, the limits of which give the principal shear directions that correspond to the lower and upper crack surface, respectively. Note from eqs. (8) that

$$x_2 = 0 \quad \rightarrow \quad \frac{\partial \psi}{\partial \phi} = 0 \quad \text{at } \phi = 0 \text{ and } \pi \tag{14}$$

The strain singularity at $x_1 = x_2 = 0$ maps to infinity in the γ-plane such that the derivatives of ψ vanish at infinity.

In elastic case, it is known that

$$x_1 - ix_2 = e^{i\phi}\left(\frac{\partial \psi}{\partial \gamma} - \frac{1}{\gamma}\frac{\partial \psi}{\partial \phi}\right) \rightarrow -\frac{1}{2\gamma}\left(\frac{k_3}{G}\right)^2 e^{-2i\phi}, \quad \gamma \rightarrow 0 \tag{15}$$

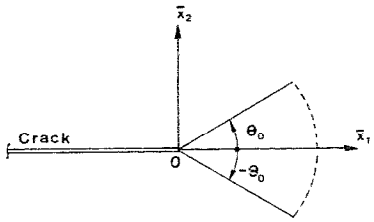

Fig. 2. Semi-infinite crack geometry.

and hence

$$\psi \sim \frac{1}{2\gamma}\left(\frac{k_3}{G}\right)^2 \cos\phi, \quad \gamma \to 0 \tag{16}$$

Because of eq. (12), the function ψ possesses a discontinuity at $\gamma = \gamma_0$ and hence the solution for $\gamma > \gamma_0$ and $\gamma < \gamma_0$ will be discussed separately.

3.1. Elliptic region ($\gamma < \gamma_0$)

A form of ψ will be selected such that the free surface crack condition will be satisfied in addition to the governing eq. (9). The choice

$$\psi = \frac{l}{2}\left\{\frac{1}{\gamma} + \gamma\left[2G\int_{\gamma_0}^{\infty}\frac{\mathrm{d}u}{u^2\tau(u)} - \gamma_0^{-2}\right]\right\}\cos\phi, \quad \gamma < \gamma_0 \tag{17}$$

is thus made. The length parameter l stands for

$$l = \left(\frac{k_3}{G}\right)^2 \tag{18}$$

with k_3 being a load intensity factor. It is expedient to introduce the quantities

$$R(\gamma) = \frac{l}{2}G\cdot\frac{1}{\gamma\tau(\gamma)}, \qquad S(\gamma) = \frac{l}{2}G\left[2\int_{\gamma}^{\infty}\frac{\mathrm{d}u}{u^2\tau(u)} - \frac{1}{\gamma\tau(\gamma)}\right] \tag{19}$$

It follows from eqs. (8) that

$$x_1 = S(\gamma_0) - R(\gamma)\cos 2\phi, \qquad x_2 = -R(\gamma)\sin 2\phi, \quad \gamma < \gamma_0 \tag{20}$$

in which

$$R(\gamma) = \frac{l}{2\gamma^2} \tag{21}$$

because of eq. (12). A system of polar coordinates $\bar{r}_1 = r_1/l$ and θ_1 in dimensionless form can thus be introduced:

$$\bar{x}_1 = \frac{3}{2\gamma_0^2} + \bar{r}_1\cos\theta_1 = \frac{3}{2\gamma_0^2} - \frac{1}{2\gamma^2}\cos 2\phi, \qquad \bar{x}_2 = \bar{r}_1\sin\theta_1 = -\frac{1}{2\gamma^2}\sin 2\phi, \quad \gamma < \gamma_0 \tag{22}$$

where $\bar{x}_i = x_j/l$. This leads to

$$\gamma = \frac{1}{\sqrt{2\bar{r}_1}}, \qquad \phi = \tfrac{1}{2}(\theta_1 + \pi) \tag{23}$$

such that

$$\bar{r}_1^2 = \left(\bar{x}_1^2 - \frac{3}{2\gamma_0^2}\right)^2 + \bar{x}_2^2, \qquad \tan\theta_1 = \frac{\bar{x}_2}{\bar{x}_1 - \dfrac{3}{2\gamma_0^2}} \tag{24}$$

Refer to Fig. 3. The region $\gamma < \gamma_0$ would correspond to that outside the circle of radius $1/2\gamma_0^2$ with center at $\bar{x}_1 = 3/2\gamma_0^2$ and $\bar{x}_2 = 0$ as given in Fig. 3. It can be seen from eqs. (22) that

$$\left(\bar{x}_1 - \frac{3}{2\gamma_0^2}\right)^2 + \bar{x}_2^2 = \frac{1}{4\gamma_0^4} \tag{25}$$

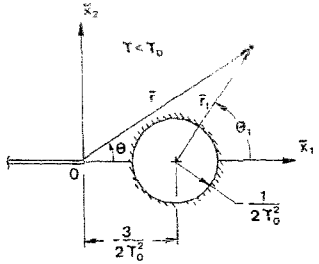

Fig. 3. Elliptic region outside circle.

3.2. *Hyperbolic region* ($\gamma > \gamma_0$)

When $d\tau/d\gamma < 0$ or $\gamma > \gamma_0$, eq. (10) is hyperbolic and hence the choice

$$\psi = lG\left[\gamma\int_{\gamma}^{\infty}\frac{du}{u^2\tau(u)}\right]\cos\phi, \quad \gamma > \gamma_0 \tag{26}$$

is made. Refer to the Appendix for the elliptic and hyperbolic character of the governing differential equations. Equations (19) become

$$x_1 = S(\gamma) - R(\gamma)\cos 2\phi, \qquad x_2 = -R(\gamma)\sin 2\phi, \quad \gamma > \gamma_0 \tag{27}$$

For the material at hand, R and S are given by

$$R(\gamma) = \frac{l}{2}\frac{1}{\gamma_0\sqrt{\gamma\gamma_0}}, \qquad S(\gamma) = \frac{3l}{2}\frac{1}{\gamma_0\sqrt{\gamma\gamma_0}}, \quad \gamma > \gamma_0 \tag{28}$$

Referring to Fig. 3, the coordinates $(\bar{r}, \theta)$ are

$$\bar{x}_1 = \bar{r}\cos\theta = \frac{1}{2\gamma_0\sqrt{\gamma\gamma_0}}(3 - \cos 2\phi), \qquad \bar{x}_2 = \bar{r}\sin\theta = -\frac{1}{2\gamma_0\sqrt{\gamma\gamma_0}}\sin 2\phi, \quad \gamma > \gamma_0 \tag{29}$$

which can be used to give

$$\sqrt{\gamma} = \frac{1}{2\bar{r}\gamma_0\sqrt{\gamma_0}}\left[3\cos\theta \pm T(\theta)\right], \quad \gamma > \gamma_0 \tag{30}$$

provided that

$$T(\theta) = \sqrt{1 - 9\sin^2\theta} \tag{31}$$

Equations (29) to (31) can be further combined to obtain

$$\begin{aligned}\cos\phi &= -2\sqrt{2}\sin\theta\left[1 + 3\sin^2\theta \pm T(\theta)\cos\theta\right]^{-1/2}\\ \sin\phi &= \frac{1}{\sqrt{2}}\left[\cos\theta \pm T(\theta)\right]\left[1 + 3\sin^2\theta \pm T(\theta)\cos\theta\right]^{-1/2}, \quad \gamma > \gamma_0\end{aligned} \tag{32}$$

The value of $\sqrt{\gamma}$ in eqs. (30) must be real and positive and this prevails if and only if

$$|\cos\theta| \geqslant \frac{2\sqrt{2}}{3}, \quad \text{for } -\theta_0 \leqslant \theta \leqslant \theta_0 \tag{33}$$

and hence $\theta_0 = \cos^{-1}(2\sqrt{2}/3)$. The region for $\gamma > \gamma_0$ is in the sector shown in Fig. 2. The positive sign in front of $f(\theta)$ in eqs. (30) and (32) is therefore taken.

3.3. Common boundary

The region in which $d\tau/d\gamma < 0$ ($\gamma > \gamma_0$) and $d\tau/d\gamma$ ($\gamma < \gamma_0$) meet at a common boundary. It can be found from the continuity of displacement and traction. Substituting eq. (17) into the first of eqs. (11) gives

$$\bar{u}_3 = \frac{u_3}{l} = -\frac{1}{\gamma}\cos\phi, \quad \gamma < \gamma_0 \tag{34}$$

while eqs. (26) and (11) render

$$\bar{u}_3 = \frac{u_3}{l} = -\frac{1}{\gamma_0}\sqrt{\frac{\gamma}{\gamma_0}}\cos\phi, \quad \gamma > \gamma_0 \tag{35}$$

Equations (23) and (34) can be combined:

$$\bar{u}_3 = \frac{1}{\sqrt{2\bar{r}_1}}\sin\left(\frac{\theta_1}{2}\right), \quad \gamma < \gamma_0 \tag{36}$$

while eqs. (30), (32) and (35) yield

$$\bar{u}_3 = \frac{1}{\sqrt{2}\bar{r}\gamma_0^3}\sin\theta \cdot \frac{[3\cos\theta + T(\theta)]^{3/2}}{[\cos\theta + T(\theta)]^{1/2}}, \quad \gamma > \gamma_0 \tag{37}$$

The common boundary that is common to the elliptic and hyperbolic region is obtained by equating eqs. (36) and (37):

$$\bar{r}\sqrt{2\bar{r}_1}\sin\frac{\theta}{2} = f(\theta) \tag{38}$$

in which

$$f(\theta) = \frac{1}{\sqrt{2}\gamma_0^3}\sin\theta \cdot \frac{[3\cos\theta + T(\theta)]^{3/2}}{[\cos\theta + T(\theta)]^{1/2}} \tag{39}$$

It can be shown that the common boundary in terms of $\bar{r}$ and θ is given by

$$\bar{r}^6\sin^2\theta + 2\bar{r}^3 f^2\cos\theta + \frac{3}{(\gamma\gamma_0)^2}f^2 - f^4 = 0 \tag{40}$$

The continuity of tractions is satisfied. Knowing that $\bar{r} = r/l$ and as $\theta \to 0$

$$r \to \frac{4}{\sqrt{3}}\frac{l}{\gamma_0^2}\sin\theta, \quad \text{on } \Gamma \tag{41}$$

where Γ denotes the common boundary in Fig. 4. It moves as the load factor $l = (k_3/G)^2$ is increased. A point such as p_1 inside Γ_1 or the hyperbolic region at one instance t_1 would be left behind as Γ_1 advances forward to Γ_L, at a time $t_2 > t_1$. Unloading would thus take place along a line such as AO in Fig. 1 with decreasing γ. The point p_1 would eventually enter into the elliptic region when the threshold (r_0, θ_0) is surpassed.

4. Unloading region

It is obvious from Fig. 4 that under increasing load, every element passes through the hyperbolic region $|\theta| < \theta_0$. Equation (36) yields $\bar{u}_3$ in the elliptic region:

$$\bar{u}_3 = \frac{\sqrt{3}}{\gamma_0} - \frac{\gamma_0}{\sqrt{3}}\bar{r}\cos\theta + O(\bar{r}^2), \quad \gamma < \gamma_0 \tag{42}$$

and eq. (37) gives $\bar{u}_3$ in the hyperbolic region:

$$\bar{u}_3 = \frac{1}{\bar{r}}\left[g(\theta) + O(\theta^3)\right], \quad \gamma > \gamma_0 \tag{43}$$

where $g(\theta) = 4\theta/\gamma_0^3$. The unloading characteristics can be summarized as:

- A hyperbolic region advances and leaves behind a region in which the elements undergo unloading. That is, when a point, say (r_a, θ_a) at A in Fig. 1, passes by (r_0, θ_0) with increasing load.
- The modulus of this unloaded region depends on the strain γ_t of the point where unloading started. Refer to eq. (12).
- The interface between the unloaded and elliptic region is a straight line tangent to the circle given by eq. (24).

4.1. Unloaded / hyperbolic interface

Suppose that $\bar{r} = h(\theta)$ describes the interface of the unloaded and hyperbolic region. If unloading starts at the point (r_a, θ_a), then

$$l = \frac{r}{h(\theta)} \tag{44}$$

Recall from eq. (43) that

$$u_3 = \frac{l^2}{r}g(\theta) \tag{45}$$

Moreover, eqs. (1) and (2) can be combined to yield

$$\gamma = \sqrt{\left(\frac{\partial u_3}{\partial r}\right)^2 + \frac{1}{r^2}\left(\frac{\partial u_3}{\partial \theta}\right)^2} \tag{46}$$

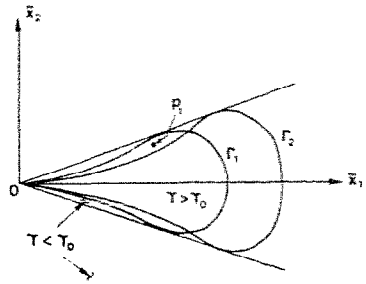

Fig. 4. Common boundary moving with increasing load.

With γ_t being the strain at (r_a, θ_a) and using eq. (44), there results

$$\gamma_t = \frac{1}{h^2(\theta)}\sqrt{\dot{g}^2(\theta) + g^2(\theta)} \tag{47}$$

where $\dot{g} = \mathrm{d}g/\mathrm{d}\theta$. Equation (47) may be inserted into (13) to give

$$G_t = \frac{G}{\gamma_0\sqrt{\gamma_0}}\left[\dot{g}^2(\theta) + g^2(\theta)\right]^{-3/4} h^3(\theta) \tag{48}$$

Equation (48) applies to any point in the unloading region.

To find u_3, use will be made of the equation of equilibrium:

$$\frac{1}{\bar{r}}\frac{\partial}{\partial \bar{r}}\left[G_t \bar{r}\frac{\partial \bar{u}_3}{\partial \bar{r}}\right] + \frac{1}{\bar{r}^2}\frac{\partial}{\partial \theta}\left[G_t \frac{\partial \bar{u}_3}{\partial \theta}\right] = 0 \tag{49}$$

A solution of $\bar{u}_3$ is in the form

$$\bar{u}_3 = w_0 + \sum_{m=1}^{\infty} \bar{r}^m w_m(\theta) \tag{50}$$

with w_0 being a constant. Let

$$h(\theta) = h_0\theta^n + \mathrm{O}(\theta^n) \tag{51}$$

Equation (51) may be put into eq. (48). This gives

$$G_t \to \tfrac{1}{8}Gh_0^3\gamma_0^3\theta^{3n}, \quad \text{as } \theta \to 0 \tag{52}$$

It can be shown by substituting eqs. (52) and (50) into eq. (49) that

$$\theta\frac{\mathrm{d}^2 w_k}{\mathrm{d}\theta^2} + 3n\frac{\mathrm{d}w_k}{\mathrm{d}\theta} + m^2\theta w_k = 0 \tag{53}$$

This is a second order ordinary linear differential equation with variable coefficients. The solution is [8]

$$w_m(\theta) = c_0\theta^{1-3n} + c_1 \tag{54}$$

for $m = 0$. Two linearly independent solutions prevail for $m \neq 0$:

$$w_m = a_m\left[1 - \frac{m^2}{2(1+3n)}\theta^2 + \cdots\right], \qquad w_m = b_m\left[\theta^{1-3n} + \frac{m^2}{6(n-1)}\theta^{3(1-n)} + \cdots\right] \tag{55}$$

in which a_m and b_m are arbitrary constants. In the limit as $\theta \to 0$, only the leading terms need to be retained:

$$w_m \to a_m + b_m\theta^{1-3n}, \quad \text{as } \theta \to 0 \tag{56}$$

If the bracket notation $[\ ]_{u/h}$ is used to denote the difference of the quantity inside across the interface of the unloaded and hyperbolic region as

$$[\ ]_{u/h} = [\ ]_u - [\ ]_h$$

then

$$[\bar{u}_3]_{u/h} = \left[\frac{\partial \bar{u}_3}{\partial \theta}\right]_{u/h} = 0 \tag{57}$$

Equations (44) and (51) may be first combined to obtain

$$\bar{r} = h_0\theta^n + O(\theta^n) \to \theta \sim \left(\frac{\bar{r}}{A}\right)^{1/n} \tag{58}$$

On the hyperbolic side of the interface, eq. (43) may be used:

$$[\bar{u}_3]_h = \frac{4\theta}{\bar{r}\gamma_0^3} + \cdots \to \frac{4}{\gamma_0^3 h_0^{1/n} A^{1/n}} \bar{r}^{\frac{1}{n}-1} + \cdots, \qquad \left[\frac{\partial \bar{u}_3}{\partial\theta}\right]_h \to \frac{4}{\gamma_0^3}\frac{1}{\bar{r}} + \cdots, \quad \gamma > \gamma_0 \tag{59}$$

Equation (50) gives $\bar{u}_3$ and $\partial\bar{u}_3/\partial\theta$ for the unloaded side:

$$\begin{aligned} [\bar{u}_3]_u &= w_0 + \sum_{m=1}^{\infty} \bar{r}^m\left(a_m + b_m\theta^{1-3n}\right) + \cdots = w_0 + a_m\bar{r}^m + b_m h_0^{3-\frac{1}{n}}\bar{r}^{m-3+\frac{1}{n}} \\ \left[\frac{\partial\bar{u}_3}{\partial\theta}\right]_u &= (1-3n)b_m\bar{r}^m\theta^{-3n} + \cdots = (1-3n)b_m h_0^3\bar{r}^{m-3} + \cdots \end{aligned} \tag{60}$$

The conditions in eqs. (57) may be imposed on eqs. (59) and (60); they give

$$\frac{4}{\gamma_0^3 A^{1/n}}\bar{r}^{\frac{1}{n}-1} = w_0 + b_m h_0^{3-\frac{1}{n}}\bar{r}^{m+3-\frac{1}{n}}, \qquad \frac{4}{\gamma_0^3}\bar{r}^{-1} = (1-3n)h_0^3\sum_{m=1}^{\infty} b_m\bar{r}^{m-3} \tag{61}$$

It follows that

$$n = 1, \qquad w_0 = \frac{4}{h_0\gamma_0^3}, \qquad b_1 = 0, \qquad b_2 = \frac{1}{(h_0\gamma_0)^3} \tag{62}$$

The anti-plane displacement in the unloaded region is thus given by

$$\begin{aligned} \bar{u}_3 &= w_0 + \bar{r}\left(a_1 - \tfrac{1}{8}a_1\theta^2 + \cdots\right) + \bar{r}^2\left(a_2 + \cdots + b_2\theta^{-2} + \cdots\right) + \cdots \quad \text{as } \theta \to 0 \\ &= w_0 + \bar{r}w_1(\theta) + \bar{r}^2 w_2(\theta) + \cdots \end{aligned} \tag{63}$$

4.2. *Unloaded / elliptic interface*

Required on the interface $\theta_0 = |\theta|$ of the unloaded and elliptic region are the conditions

$$[\bar{u}_3]_{u/e} = \left[\frac{\partial\bar{u}_3}{\partial\theta}\right]_{u/e} = 0 \tag{64}$$

On the side of the elliptic region, eq. (42) prevails while on the unloaded side, eq. (63) applies. These expressions may be substituted in the first of eqs. (64) for $\theta = \theta_0 \to 0$:

$$w_0 + \bar{r}w_1(\theta_0) + \bar{r}^2 w_2(\theta_0) + \cdots = \frac{\sqrt{3}}{\gamma_0} - \frac{\gamma_0\bar{r}}{\sqrt{3}}\cos\theta_0 + \cdots \tag{65}$$

Equating coefficients for like power of $\bar{r}$, w_0 and $w_1(\theta_0)$ are found:

$$w_0 = \frac{\sqrt{3}}{\gamma_0}, \qquad w_1(\theta_0) = -\frac{\gamma_0}{\sqrt{3}} \tag{66}$$

The value w_0 may be used to express h_0 and b_2 in eq. (62) in terms of γ_0:

$$h_0 = \frac{2\sqrt{3}}{\gamma_0^2}, \qquad b_2 = -\frac{\gamma_0^3}{12\sqrt{3}} \tag{67}$$

The condition $[\partial \bar{u}_3/\partial\theta]_{u/e}$ in eq. (64) would only yield relations for higher order terms and would not be considered.

5. Summary and discussion of results

For a material that behaves linearly to a peak and then softens in proportion to the inverse square root of the strain, the stress and strain state near a semi-infinite crack in out-of-plane shear consist of three regions. They could be referred to as the unloaded, hyperbolic and elliptic region. The asymptotic values of τ_{ij} and γ_{ij} are obtained for $G = 10^6$ kg/cm^2 and $\gamma_0 = 1$. Remember that $l = (k_3/G)^2$ with k_3 being the elastic Mode III crack-tip stress intensity factor.

5.1. Unloaded region

The local strains are

$$\begin{Bmatrix} \gamma_{r3} \\ \gamma_{\theta 3} \end{Bmatrix} = -\frac{\bar{r}\gamma_0^3}{6\sqrt{3}} \begin{Bmatrix} \theta^{-2} \\ \theta^{-3} \end{Bmatrix} = 0.1\bar{r} \begin{Bmatrix} \theta^{-2} \\ \theta^{-3} \end{Bmatrix}, \quad \text{as } \theta \to 0 \tag{68}$$

Similarly, the local stresses take the forms

$$\begin{Bmatrix} \tau_{r3} \\ \tau_{\theta 3} \end{Bmatrix} = \frac{G\bar{r}}{2} \begin{Bmatrix} -\theta \\ 1 \end{Bmatrix} = 5 \times 10^5 (\bar{r}) \begin{Bmatrix} -\theta \\ 1 \end{Bmatrix}, \quad \theta \to 0 \tag{69}$$

The modulus of the unloaded material is

$$G_t = 3\sqrt{3}\, G \left\{ \frac{\theta}{\gamma_0} \right\}^3, \quad \theta \to 0 \tag{70}$$

Both γ_{ij} and τ_{ij} depend linearly on the radial distance r from the crack tip. That is, unloading effect diminishes as the crack tip is approached.

5.2. Hyperbolic region

The stresses and strains in this region will increase with load in contrast to the situation in the unloaded region. Local strains are given by

$$\begin{Bmatrix} \gamma_{r3} \\ \gamma_{\theta 3} \end{Bmatrix} = \frac{4}{\gamma_0^3 \bar{r}^2} \begin{Bmatrix} -\theta \\ 1 \end{Bmatrix} = \frac{4}{\bar{r}^2} \begin{Bmatrix} -\theta \\ 1 \end{Bmatrix}, \quad \theta \to 0 \tag{71}$$

This implies that the displacement $\bar{u}_3 = O(\theta/\bar{r})$ would be singular as $\bar{r} \to 0$. However, the hyperbolic region is limited by the boundary $\bar{r} \sim 2\sqrt{3}\,\theta/\gamma_0^2$ and hence $\bar{u}_3 = O(1)$ is finite. The stresses are nonsingular:

$$\begin{Bmatrix} \tau_{r3} \\ \tau_{\theta 3} \end{Bmatrix} = \frac{G\gamma_0^{3/2}}{2} \bar{r} \begin{Bmatrix} -\theta \\ 1 \end{Bmatrix} = 5 \times 10^5 (\bar{r}) \begin{Bmatrix} -\theta \\ 1 \end{Bmatrix}, \quad \theta \to 0 \tag{72}$$

Hence, the stress intensification for a nonlinear material is not the same as that of strain.

5.3. Elliptic region

In the elliptic region, the stresses and strains are independent of the distance from the crack; they vary only with the angle θ. They are given by

$$\begin{Bmatrix} \gamma_{r3} \\ \gamma_{\theta 3} \end{Bmatrix} = \frac{\gamma_0}{\sqrt{3}} \begin{Bmatrix} -\cos\theta \\ \sin\theta \end{Bmatrix} = 0.58 \begin{Bmatrix} -\cos\theta \\ \sin\theta \end{Bmatrix} \tag{73}$$

and

$$\begin{Bmatrix} \tau_{r3} \\ \tau_{\theta 3} \end{Bmatrix} = \frac{G\gamma_0}{\sqrt{3}} \begin{Bmatrix} -\cos\theta \\ \sin\theta \end{Bmatrix} = 5.8 \times 10^5 \begin{Bmatrix} -\cos\theta \\ \sin\theta \end{Bmatrix} \tag{74}$$

5.4. Concluding remarks

Equations (71) to (74) inclusive show that the stresses and strains ahead of a crack are nonhomogeneous, i.e., their r and θ dependence are different and dictated by the assumed form of the constitutive relation. The single parameter stress intensity factor concept in elastic fracture mechanics therefore no longer holds in plasticity. There is the need to elaborate on how to establish the threshold of material damage in relation to solution obtained from the theory of plasticity.

Acknowledgement

This work was supported by the China National Natural Science Foundation of the People's Republic of China under contract No. 19072055.

Appendix

The differential equation governing the strain function ψ has a dual character in that it is elliptic when $d\tau/d\gamma > 0$ and hyperbolic when $d\tau/d\gamma < 0$. To show this, consider $x_i(\tau_{ij}, \gamma_{ij})$ and $x_i(\tau_{ij}, \tau_{ij})$ such that

$$\frac{\partial x_i}{\partial \tau_{jk}} = \frac{\partial x_i}{\partial \tau_{lk}} \frac{\partial \tau_{lk}}{\partial \tau_{jk}} = A_{il}\, \delta_{jk}, \quad i, j, k = 1, 2 \tag{A.1}$$

Now for $i = 1, 2$ and $j = 1$, there results

$$\frac{\partial x_2}{\partial \tau_{21}} = \Delta \frac{\partial \tau_{12}}{\partial x_1}, \qquad \frac{\partial x_1}{\partial \tau_{11}} = -\Delta \frac{\partial \tau_{22}}{\partial x_2} \tag{A.2}$$

in which

$$\Delta = \begin{vmatrix} \dfrac{\partial x_1}{\partial \tau_{12}} & \dfrac{\partial x_1}{\partial \tau_{22}} \\ \dfrac{\partial x_2}{\partial \tau_{12}} & \dfrac{\partial x_2}{\partial \tau_{22}} \end{vmatrix} \tag{A.3}$$

Similarly, if $i = 1, 2$ and $j = 2$, eqs. (A.1) give

$$\frac{\partial x_1}{\partial \tau_{22}} = -\Delta \frac{\partial \tau_{12}}{\partial x_2}, \qquad \frac{\partial x_1}{\partial \tau_{12}} = \Delta \frac{\partial \tau_{22}}{\partial x_2} \tag{A.4}$$

It can be deduced from the first of eqs. (A.2) and second of eqs. (A.4) that

$$\frac{\partial x_2}{\partial \tau_{23}} + \frac{\partial x_1}{\partial \tau_{13}} = \Delta\left(\frac{\partial \tau_{13}}{\partial x_1} + \frac{\partial \tau_{23}}{\partial x_2}\right) = 0 \tag{A.5}$$

as a result of eq. (4) since $\Delta = 0$. Equations (6) may be substituted into eq. (A.5) to yield

$$\frac{\partial}{\partial \tau_{23}}\left(\frac{\partial \psi}{\partial \gamma_{23}}\right) + \frac{\partial}{\partial \tau_{13}}\left(\frac{\partial \psi}{\partial \gamma_{13}}\right) = 0 \tag{A.6}$$

and hence

$$\frac{\partial \gamma_{j3}}{\partial \tau_{23}}\left(\frac{\partial^2 \psi}{\partial \gamma_{j3}\partial \gamma_{23}}\right) + \frac{\partial \gamma_{j3}}{\partial \tau_{13}}\left(\frac{\partial^2 \psi}{\partial \gamma_{j3}\partial \gamma_{13}}\right) = 0 \tag{A.7}$$

The property of proportional loading in eq. (3) may be invoked:

$$\begin{aligned}\frac{\partial \gamma_{j3}}{\partial \tau_{i3}} &= \frac{\partial}{\partial \tau_{i3}}\left(\frac{\gamma}{\tau}\tau_{j3}\right) = \frac{1}{\tau_2}\left\{-\gamma\tau_{j3}\frac{\tau_{i3}}{\tau} + \tau\left[\frac{\partial \tau}{\partial \tau_{i3}}\frac{\mathrm{d}\gamma}{\mathrm{d}\tau}\tau_{j3} + \gamma\delta_{ij}\right]\right\} \\ &= \frac{\gamma}{\tau}\delta_{ij} + \frac{\tau_{i3}\tau_{j3}}{\tau^3}\left(\tau\frac{\mathrm{d}\gamma}{\mathrm{d}\tau} - \gamma\right)\end{aligned} \tag{A.8}$$

Under these considerations, eq. (A.7) can be written as

$$A\frac{\partial^2 \psi}{\partial \gamma_{13}^2} + B\frac{\partial^2 \psi}{\partial \gamma_{13}\partial \gamma_{23}} + C\frac{\partial^2 \psi}{\partial \gamma_{23}^2} = 0 \tag{A.9}$$

in which A, B and C stand for

$$A = \frac{\gamma}{\tau} + \frac{\tau_{13}^2}{\tau^3}f(\tau), \qquad B = \frac{2\tau_{13}\tau_{23}}{\tau^3}f(\tau), \qquad C = \frac{\gamma}{\tau} + \frac{\tau_{23}^2}{\tau^3}f(\tau) \tag{A.10}$$

The function $f(\tau)$ takes the form

$$f(\tau) = \tau\frac{\mathrm{d}\gamma}{\mathrm{d}\tau} - \gamma \tag{A.11}$$

To test whether eq. (A.9) is elliptic or hyperbolic, the quantity $B^2 - 4AC$ is computed

$$B^2 - 4AC = \frac{4\tau_{13}^2\tau_{23}^2}{\tau^6}f^2 - 4\left(\frac{\gamma}{\tau} + \frac{\tau_{13}^2}{\tau^3}f\right)\left(\frac{\gamma}{\tau} + \frac{\tau_{23}^2}{\tau^3}f\right) = -4\frac{\gamma}{\tau}\frac{\mathrm{d}\gamma}{\mathrm{d}\tau} \tag{A.12}$$

As both τ and γ are positive, the sign of $B^2 - 4AC$ depends on whether $\mathrm{d}\tau/\mathrm{d}\gamma$ is positive or negative. This determines whether eq. (A.9) is elliptic ($\mathrm{d}\tau/\mathrm{d}\gamma < 0$) or hyperbolic ($\mathrm{d}\tau/\mathrm{d}\gamma > 0$).

References

[1] G.C. Sih and E. Madenci, Crack growth resistance characterized by the strain energy density function, *J. Eng. Fract. Mech.* 18 (6) (1983) 1159–1171.

[2] G.C. Sih and E. Madenci, Fracture initiation under gross yielding: strain energy density criterion, *J. Eng. Fract. Mech.* 18 (1983) 667–677.

[3] G.C. Sih and D.Y. Tzou, Plastic deformation and crack growth behavior, *Plasticity and Failure Behavior of Solids*, edited by G.C. Sih, A.J. Ishlinsky and S.T. Mileiko (Kluwer Academic Publishers: The Netherlands, 1990) pp. 91–114.

[4] J.K. Knowles and E. Sternberg. Discontinuous deformation gradients near the tip of a crack in finite anti-plane shear: an example, *J. Elasticity 10* (1) (1980) 81–110.
[5] T.H. Hao, Nonlinear response of anti-plane shear crack, *Theoret. Appl. Fract. Mech. 9* (1988) 255–262.
[6] A. Carpinteri and G.C. Sih, Damage accumulation and crack growth in bilinear materials with softening: application of strain energy density theory, *Theoret. Appl. Fract. Mech. 1* (2) (1984) 145–159.
[7] L.M. Kachanov, *Introduction to Continuum Damage Mechanics* (Martinus Nijhoff Publishers: Dordrecht, The Netherlands, 1986).